Magnetic circular dichroism and optical detection of electron paramagnetic resonance of the Sb_{Ga} heteroantisite defect in GaAs:Sb

P. Omling and D. M. Hofmann
Department of Solid State Physics, University of Lund, Box 118, S-221 00 Lund, Sweden

M. Kunzer, M. Baeumler, and U. Kaufmann
Fraunhofer-Institute for Applied Solid State Physics, Tullastrasse 72, D-7800 Freiburg, Federal Republic of Germany
(Received 16 August 1991)

In an investigation of GaAs doped with Sb to a concentration of $\approx 1\times10^{19}$ cm^{-3}, the electron-paramagnetic-resonance (EPR) signal of the Sb_{Ga} heteroantisite defect has been optically detected by monitoring the microwave-induced changes in the magnetic-circular-dichroism (MCD) absorption signal. All hyperfine transitions expected for the two Sb isotopes (^{121}Sb and ^{123}Sb) were observed and the identification of the Sb_{Ga} defect is thus confirmed. The g value is 2.02 and the hyperfine constants are 0.220 cm^{-1} (for ^{121}Sb) and 0.120 cm^{-1} (for ^{123}Sb). The MCD signal of the Sb_{Ga} defect has been measured being tagged to the EPR signal, and a comparison with the corresponding spectrum for the As_{Ga}(EL2) defect is made. The existing models fail to give a satisfactory explanation for the MCD spectra.

I. INTRODUCTION

The antisite defects in GaAs are interesting objects to study in semiconductor physics because of their important roles in technology, their fascinating physical properties, and, sometimes, their evasive nature when it comes to identification.[1-3] Of the native antisite defects the Ga_{As} seems to form a simple double acceptor[4,5] and the As_{Ga} has been observed in several different atomistic configurations.[2] Of those configurations the one related to the double donor EL2 is by far the most investigated because of its role in semi-insulating GaAs and its metastable behavior.[3]

The existence of heteroantisite defects, i.e., a group-III impurity on the group-V sublattice or a group-V impurity on the group-III sublattice, was demonstrated by the detection of the B_{As} defect. This defect was identified by local vibrational-mode spectroscopy,[6,7] but no energy level has been observed in the band gap. More recently, the existence of an energy level related to the Sb_{Ga} heteroantisite defect was tentatively inferred from Hall-effect measurements on GaAs crystals doped with Sb in the 1×10^{19} cm^{-3} range.[8] The strength of the argument was later significantly increased by electron-paramagnetic-resonance (EPR) measurements on the same crystals.[9] The EPR spectrum showed four lines which were explained as being due to the Sb_{Ga}^{+} charge state of the double-donor heteroantisite defect, where the magnitude of the hyperfine interaction in comparison with the applied microwave frequency (9.5 GHz) prevented observation of all the fourteen expected lines. A later photo-EPR investigation[10] correlated the EPR spectrum with the E_c-05 eV energy level detected in the Hall-effect measurements. Recently, the Sb_{Ga} defect was suggested to be observed also in metalorganic vapor phase epitaxial GaAs.[11]

The purpose of this work is to present a complete EPR spectrum of the Sb_{Ga} heteroantisite defect, and thus to confirm the identification of the defect. In order to do this we have applied an optically detected EPR technique, where we first measure the magnetic-circular dichroism (MCD) of the absorption of the Sb_{Ga} defect. The change of this signal as a function of magnetic field is then studied during a double-resonance experiment using 24-GHz microwaves. According to previous EPR results (Ref. 9), this microwave energy should allow all the expected transitions to be observed in a suitable magnetic field range. In addition, due to the combination of spin resonance and optical techniques we gain insight into the absorption transitions of the Sb_{Ga} defects by measuring the EPR signal as a function of the optical excitation energy. This excitation technique has been previously applied to the As_{Ga}(EL2) (Ref. 12) and other As_{Ga} defects,[2] and a comparison with those spectra may be helpful for an understanding of the optical transitions responsible for the MCD signal.

II. EXPERIMENTAL DETAILS

The MCD and the optically detected EPR experiments were performed at pumped-liquid-He temperatures in a Magnex 4T superconducting magnet optical cryostate. The samples were mounted in a 24-GHz TE_{011} cavity with large openings for optical access. The right- and left-circularly polarized components of the light were produced by dispersion of light from a 250-W tungsten lamp in a Spex 1681 monochromator, and after the monochromatic light was passed through an achromatic linear polarizer the right- and left-circularly-polarized light was produced by a Hinds PEM quartz modulator operating at 42 kHz. The light transmitted through the sample (and parallel to the magnetic field) was focused on a cooled Ge detector (North Coast).

In the MCD experiments the difference in absorption

between right- and left-circularly-polarized light, $\alpha_L - \alpha_R$, is measured at a fixed magnetic field. The MCD signal in absorption can be defined as[13]

$$\alpha_L - \alpha_R = 2(I_R - I_L)/[(I_R + I_L)d] , \quad (1)$$

where I_L and I_R are the transmitted light intensities for left- (L) and right- (R) circularly-polarized light, respectively, and d is the thickness of the sample. In Eq. (1) it is assumed that $(\alpha_L - \alpha_R)d \ll 1$, which was the case in our experiments. In order to directly measure $\alpha_L - \alpha_R$ a double lock-in technique was used. One signal, detected in phase with the 42-kHz modulator, was proportional to $(I_L - I_R)$, and a second signal, detected in phase with an optical chopper operating at ≈ 200 Hz, was proportional to the total intensity $(I_L + I_R)$. The two signals were divided, and as a result also the spectral responses from light source, monochromator, detector, etc., were corrected automatically. In the optically detected EPR experiments the microwave-induced changes of the MCD signal were measured as a function of magnetic field. When the microwaves induce an EPR transition in the Zeeman-split ground state, the Boltzmann-distributed population differences in these energy levels equalize and the intensity of the MCD signal decreases, thus indicating the resonances.

The sample used in this investigation is sample A used in the previous EPR and photo-EPR investigations.[9,10] In short, this GaAs crystal has been grown by the liquid-encapsulated Czochralski technique and is doped to a level $\approx 1\times10^{19}$ cm^{-3} with the isovalent impurity Sb. The crystal contains two deep donors, the As_{Ga}(EL2) with its $0/+$ level at midgap and the (assumed) Sb_{Ga} defect with its $0/+$ transition at $E_c - 0.5$ eV, both in the concentration range $(1-2)\times10^{16}$ cm^{-3}.

III. EXPERIMENTAL RESULTS AND ANALYSIS

As was shown in Ref. 10, the As_{Ga}(EL2) and the Sb_{Ga} defects can exchange electrons and holes upon strong optical illumination. For instance, by preilluminating the sample with 1.46-eV photons the $[As_{Ga}(EL2)]^+$ and $Sb_{Ga}{}^0$ charge states were created. Of those, only the first is MCD active. The MCD spectrum of As_{Ga}(EL2) obtained in this way is shown in Fig. 1 [denoted As_{Ga}(EL2)] and agrees with the As_{Ga}(EL2) MCD spectra published previously.[12] If the MCD spectrum was measured without preillumination, a more complicated spectrum appeared [denoted As_{Ga}(EL2)+Sb_{Ga} in Fig. 1]. Finally, by illuminating the sample with 1.18-eV photons the As_{Ga}(EL2) antisites are persistently quenched[3] and only the $Sb_{Ga}{}^+$ charge state is present in the sample. The MCD spectrum obtained in this condition is denoted Sb_{Ga} in Fig. 1.

The microwave-induced changes of the MCD signal as observed by monitoring at $h\nu = 1.4$ eV and sweeping the magnetic field are shown in Fig. 2 [the curve denoted As_{Ga}(EL2)]. It shows the well-known EPR spectrum from the $As_{Ga}{}^+$(EL2) antisite defect[12] with electron spin $S = \frac{1}{2}$ and nuclear spin $I(\mathrm{As}) = \frac{3}{2}$. If the same experiment is performed on the "Sb_{Ga}" MCD signal at $h\nu = 0.8$ eV a more complex spectrum, denoted Sb_{Ga} in Fig. 2, appears. In Fig. 3 the new EPR spectrum has been uncovered by subtracting the "Sb_{Ga}" spectrum in Fig. 2 from the corresponding spectrum measured without microwaves.

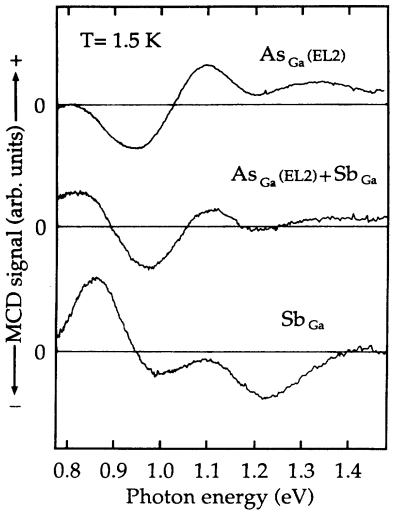

FIG. 1. By preilluminating the sample with different photon energies different charge states of the Sb_{Ga} and the As_{Ga}(EL2) defects could be occupied. The figure shows the MCD spectra obtained after preillumination using $h\nu = 1.46$ eV (top spectrum), no preillumination (middle spectrum), and after photoquenching of the As_{Ga}(EL2) defect using $h\nu = 1.18$ eV photons (bottom spectrum).

The isotropic EPR spectrum in Fig. 3 was analyzed in the model suggested for the $Sb_{Ga}{}^+$ heteroantisite in GaAs.[9] Using $S = \frac{1}{2}$ and the natural abundance of the Sb isotopes (57% ^{121}Sb with $I = \frac{5}{2}$ and 43% ^{123}Sb with $I = \frac{7}{2}$) the spin Hamiltonian can be written as

$$H = \mu_B \mathbf{B}\cdot\mathbf{g}\cdot\mathbf{S} + \mathbf{S}\cdot\mathbf{A}_{^{121}\mathrm{Sb}}\cdot\mathbf{I}(^{121}\mathrm{Sb}) + \mathbf{S}\cdot\mathbf{A}_{^{123}Sb}\cdot\mathbf{I}(^{123}Sb) . \quad (2)$$

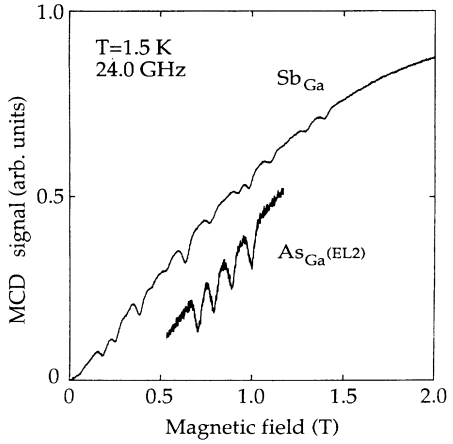

FIG. 2. The microwave-induced changes of the MCD signal when monitoring at $h\nu = 1.40$ eV show the As_{Ga}(EL2) EPR spectrum. When monitoring at $h\nu = 0.8$ eV a more complicated EPR spectrum related to Sb_{Ga} appears.

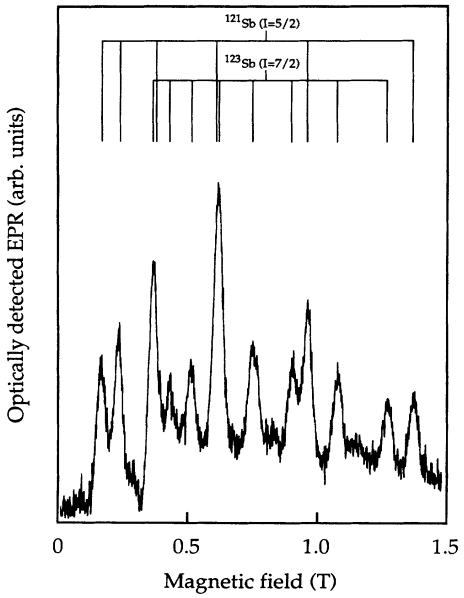

FIG. 3. Subtracting the "Sb_{Ga}" MCD spectrum in Fig. 2 from the corresponding spectrum obtained without microwaves reveals the Sb_{Ga} EPR spectrum. The stick spectra show the calculated peak positions for the two Sb isotopes (natural abundances: ^{121}Sb 57% and ^{123}Sb 43%) using Eq. (2) and $g=2.02$, $A_{^{121}Sb}=0.220\ cm^{-1}$, and $A_{^{123}Sb}=0.120\ cm^{-1}$.

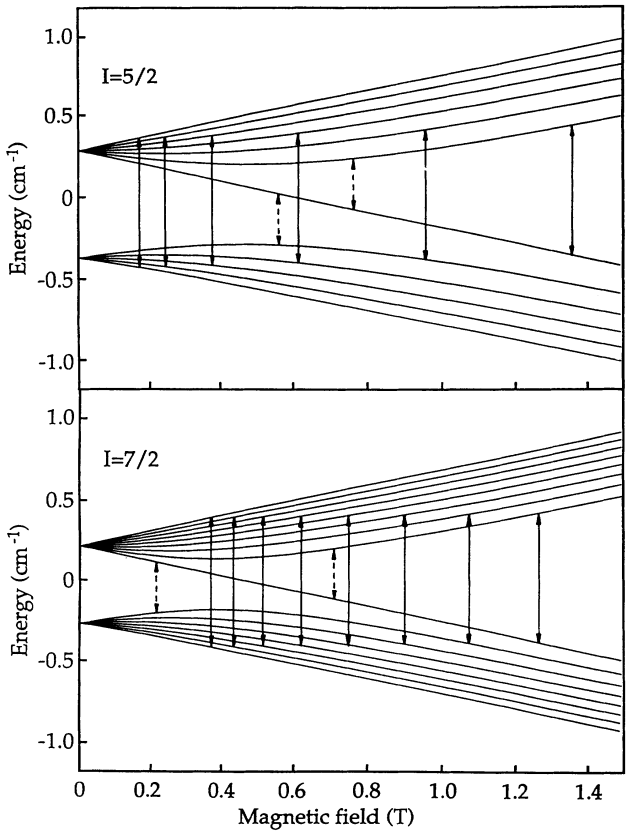

FIG. 4. Zeeman splittings of the Sb_{Ga}^{+} ground states for the isotopes ^{121}Sb and ^{123}Sb as obtained from the exact solution of Eq. (2). The EPR transitions observed at 24.0 GHz are indicated by solid arrows (this work) and those observed at 9.5 GHz are indicated by dashed arrows (Ref. 9).

Here the second and third terms denote the hyperfine interaction with the central Sb atoms and the symbols have their usual meanings. In zero magnetic field the hyperfine interaction splits the ground state of the Sb_{Ga}^{+} defect into $F=2$ and 3 ($I=\frac{5}{2}$) and $F=3$ and 4 ($I=\frac{7}{2}$) (here $F=I\pm S$ where F is the total angular momentum). When the magnetic field is applied these energy levels are Zeeman split, and the corresponding energy-level diagram can be directly calculated from Eq. (2). From such a calculation, using $g=2.02$ and the central Sb hyperfine splittings $A_{^{121}Sb}=0.220\ cm^{-1}$ and $A_{^{123}Sb}=0.120\ cm^{-1}$, the experimental spectrum can be satisfactorily explained. The resulting magnetic-field positions for the EPR transitions for the two isotopes are indicated in Fig. 3. The resulting energy-level diagrams for the two isotopes are shown in Fig. 4. Here the 24-GHz microwave transitions are drawn as solid lines.

As mentioned before, in the previous EPR investigation[9] at 9.5 GHz only four of these transitions were observed. However, the g value and the hyperfine splittings deduced from these four lines agree with those determined in the present investigation, and the 9.5-GHz transitions have been included as dashed lines in Fig. 4. Based on the arguments presented in Ref. 9 for the identification of the EPR spectrum as originating in the Sb_{Ga} heteroantisite defect, the present observation of all the Sb hyperfine lines, and the agreement between the results obtained using the two microwave frequencies, we conclude that the Sb_{Ga} defect is hereby identified. A slight offset of the Sb_{Ga} from the perfect substitutional position might be possible, despite the fact that no such indication is obtained from the experiments. The effect has to be hidden in the linewidth of the EPR lines which is caused by ligand hyperfine interaction of neighboring As and Ga nuclei.

The spectral dependence of the Sb_{Ga} MCD signal was measured by detecting the magnitude of one of the Sb_{Ga} EPR lines as the wavelength was scanned. This excitation spectrum (tagged MCD) is identical to the "Sb_{Ga}" spectrum shown in Fig. 1. It is now obvious that the middle spectrum in Fig. 1 is a superposition of the MCD spectra from As_{Ga}(EL2) and Sb_{Ga}.

IV. DISCUSSION

A definite assignment of the optical transition giving rise to the Sb_{Ga} MCD spectrum in Fig. 1 is difficult. However, due to the paramagnetic nature of this MCD, it is certain that the initial state of the transition is the $^2A_1$ ground state of the singly ionized Sb_{Ga} donor, Sb_{Ga}^{+}. Internal as well as ionizing optical transitions involving this ground state can give rise to MCD absorption bands. In the case of As_{Ga} (EL2) the internal $^2A_1 \rightarrow {}^2T_2$ transition of As_{Ga}^{+} was originally thought to be responsible for the MCD.[12] This model can qualitatively account for the As_{Ga}(EL2) MCD shape only if there were two T_2 levels or, alternatively, one T_2 level with a large negative ($3\lambda/2 \approx -0.35$ eV) spin-orbit splitting within the excited $^2T_2$ states (Γ_8 below Γ_7) and where the Γ_8 spin-orbit level is split by an axial perturbation. To date a band-shape

calculation to support that model has not been performed and the negative spin-orbit coupling constant that would be required is not understood. Alternatively it has been suggested that the As_{Ga}(EL2) MCD spectrum results from photoneutralization of As_{Ga}^{+}, i.e., $As_{Ga}^{+}+h\nu \rightarrow As_{Ga}^{0}+$ hole. This model is strongly supported by the fact that it can explain the overall MCD line shape with only one fitting parameter.[14,15]

Neither of the above models, when applied to Sb_{Ga}, can directly explain the Sb_{Ga} MCD line shape. In the internal-transition model, a positive spin-orbit coupling constant within $^2T_2$ would be required to understand that the Sb_{Ga} MCD peaks at 0.87 and 1.22 eV have a positive and a negative sign, respectively. This is consistent with the expected sign of the spin-orbit splitting but its magnitude is less than the expected one (the spin-orbit splitting in Sb-containing III-V compounds is ≈ 0.7 eV, i.e., two times the splitting in GaAs). Furthermore, the negative MCD peak at 0.99 eV cannot be explained unless the Γ_8 spin-orbit state is split by a perturbation of lower-than-axial symmetry.[16] On the other hand, the hole excitation model ($Sb_{Ga}^{+} \rightarrow Sb_{Ga}^{0}+$ hole) also cannot account for all Sb_{Ga} MCD peaks. Since the (0/+) Sb_{Ga} donor level is at $E_v+1.0$ eV it predicts only one negative MCD peak which could correspond to the 1.22-eV peak in Fig. 1. If in addition the photoionization process $Sb_{Ga}^{+} \rightarrow Sb_{Ga}^{2+}+$ electron is considered this should induce a positive MCD peak with an onset near 0.75 eV since the (+/2+) Sb_{Ga} donor level has been found to be at $E_c-0.75$ eV.[17] Thus this transition could be related to the 0.87-eV peak in the Sb_{Ga} MCD spectrum, but the negative peak at 0.99 eV again remains unexplained. These considerations show that neither model gives a satisfactory qualitative explanation for the Sb_{Ga} MCD line shape. However, a combination of both intradefect and ionization transitions should be able to explain the observed MCD line shape, but further work on the MCD band modeling is required.

ACKNOWLEDGMENTS

This work was supported by the Swedish Natural Sciences Research Council and the Swedish Board for Technical Developments.

[1]H. J. von Bardeleben and B. Pajot, Rev. Phys. Appl. (France) **23**, 727 (1988).

[2]B. K. Meyer, in *Defects in Semiconductors,* Vols. 38–41 of *Material Science Forum,* edited by G. Ferenczi (Trans Tech, Aedermannsdorf, Switzerland, 1988), p. 59.

[3]For a review, see G. M. Martin and S. Makram-Ebeid, in *Deep Centers in Semiconductors,* edited by S. T. Pantelides (Gordon and Breach, New York, 1985), p. 399.

[4]P. W. Yu, W. C. Mitchel, M. G. Mier, S. S. Li, and W. L. Wang, Appl. Phys. Lett. **41**, 532 (1982).

[5]M. Mikara, M. Mannoh, K. Shinozaki, S. Naritsuka, and M. Ishii, Jpn. J. Appl. Phys. **25**, L611 (1986).

[6]J. Woodhead, R. C. Newman, I. Grant, D. Rumsby, and R. M. Ware, J. Phys. C **16**, 5523 (1983).

[7]D. W. Fischer and P. W. Yu, J. Appl. Phys. **59**, 1952 (1986).

[8]W. C. Mitchel and P. W. Yu, J. Appl. Phys. **62**, 4781 (1987).

[9]M. Baeumler, J. Schneider, U. Kaufmann, W. C. Mitchel, and P. W. Yu, Phys. Rev. B **39**, 6253 (1989).

[10]M. Baeumler, F. Fuchs, and U. Kaufmann, Phys. Rev. B **40**, 8072 (1989).

[11]R. Yakimova, P. Omling, B. H. Yang, L. Samuelson, J.-O. Fornell, and L. Ledebo, Appl. Phys. Lett. **59**, 1323 (1991).

[12]B. K. Meyer, J.-M. Spaeth, and M. Scheffler, Phys. Rev. Lett. **52**, 851 (1984).

[13]L. F. Mollenauer and S. Pan, Phys. Rev. B **6**, 772 (1972).

[14]U. Kaufmann and J. Windscheif, Phys. Rev. B **38**, 10060 (1988).

[15]U. Kaufmann and J. Windscheif, in *Semiinsulating III–V Materials,* edited by G. Grossmann and L. Ledebo (Hilger, Bristol, 1988), p. 343.

[16]M. C. M. O'Brien, J. Phys. C **18**, 4963 (1985).

[17]P. Omling, B. H. Yang, L. Samuelson, R. Yakimova, J.-O. Fornell, and L. Ledebo, Phys. Rev. B **44**, 13 398 (1991).